

## ENCIT-2018-0009

### FORECASTING THE LENGTH OF THE UNDEVELOPED FLOW REGION IN THE INLET OF ASYMMETRIC BIFURCATIONS II

#### Flavio Peres Amado

Universidade Estácio de Sá, Rua Eduardo Luiz Gomes, 134 - Morro do Estado, Niterói - RJ, 24020-340  
e-mails: flavioam@petrobras.com.br; fpamado@live.estacio.com.br

#### Mila Rosendarl Avelino

Universidade do Estado do Rio de Janeiro – UERJ, Cx. Postal 68503, Rio de Janeiro - RJ, 21945-970;  
e-mail: mila.avelino@pq.cnpq.br

#### Jordana Colman

Universidade Federal do Rio de Janeiro – UFRJ, Centro de Tecnologia - Av. Horácio Macedo, 2030, Cidade Universitária, Rio de Janeiro - RJ, 21941-450  
e-mail: jordanacolman@yahoo.com.br

#### Ediomedson Sales de Lucena

#### Narcisio Gragory dos Santos Mazzarela

Universidade Estácio de Sá, Rua Eduardo Luiz Gomes, 134 - Morro do Estado, Niterói - RJ, 24020-340  
e-mails: ediomedson@hotmail.com, narcisio.gregory@gmail.com

**Abstract.** In the paper named "Forecasting the Length of the Undeveloped Flow Region in the Inlet of Asymmetric Bifurcations I", also presented to this congress, an equation of prediction of the length of the not fully developed flow region in asymmetric bifurcations is proposed. However, only the variation of the bifurcation angles and flow rates, for a pipe with 20 mm in diameter, are evaluated. In this work, it is intended to complement this first manuscript with results acquired from simulations where the diameter of the tube is varied. Constants and exponents are calculated from the measurement of the region of interest in the images generated via CFD. Thus, a more complete equation is obtained, with values collected from the variation of all the quantities that influence the phenomenon. The development of a prediction equation for the thermal entrance length, in a method similar to the present one, is recommended to complete the study of the entrance region in bifurcations.

**Keywords:** flow development, bifurcations

## 1. INTRODUCTION

In flows that need to be laminar, a lot of obstacles may cause unwanted turbulence. A new not fully developed flow region will appear whenever there are valves, bends, bifurcations, and other restrictions in the flow path. Several studies have proposed equations that intend to predict the extent of this turbulence in curves and helicoids of conventional or thin pipe (Austin and Seader 1974; Newson and Hodgson, 1974; Yao and Berger, 1975; Agrawal et al, 1978; Soh, and Berger, 1984; So et al. 1991; Srpingger et al, 2009), in symmetric bifurcations of microchannels (Amado et al 2018a), in asymmetric bifurcations of pipe with 20 mm in diameter (Amado et al 2018b) and other schemes.

Some authors have postulated equations in angular length format. Austin and Seader, 1974, have presented Eq. (1), which intends to predict the size of the flow-developing region in curved tubes, expressed in terms of an angle  $\varphi$ , which varies as a function of the radius of curvature,  $R$ , and the internal radius  $a$ , as well as the Dean Number,  $De$ . However, most authors, like Srpingger et al., 2009, present their equations in the format of Eq. (2), where  $Re$  is the Reynolds Number and  $D$ , the inner diameter of the tube.

$$\varphi = 49 \left( De \frac{a}{R} \right)^{0.33} \quad (1)$$

$$L = k (2R)^m Re^n D^p \quad (2)$$

For the case of Eq. (2), constants  $k$ ,  $m$ ,  $n$  and  $p$  have to be found, according to the shape of the stretch whose length of the flow development region is to be predicted and depending on the fluid properties and flow characteristics.

## 2. MATERIALS AND METHODS

As a complementary work to the article submitted to this ENCIT2018, under the heading "Forecasting the Length of the Undeveloped Flow Region in the Inlet of Asymmetric Bifurcations I" (Amado et al, 2018a), the intention of this manuscript is to complete the results presented there. In this sense, flow simulations were performed seeking represent asymmetric bifurcations with variation in the pipe diameter, but maintaining constant the half-angles of the forks (30 ° and 45 °) as well as the fluid flow rate  $Q$  ( $2.78 \times 10^{-9} \text{ m}^3/\text{s}$  of water in NTP conditions).

### 2.1 Simulation Strategy

The simulation strategy used was the same as that adopted in Amado et al, 2018a. Implementations in finite difference method and in a commercial package were carried out with the purposes of comparing and check the appearance of the region of interest and measure it. The image is expected to have an aspect similar to the scheme shown in Fig. 1 (Amado et al, 2018b).

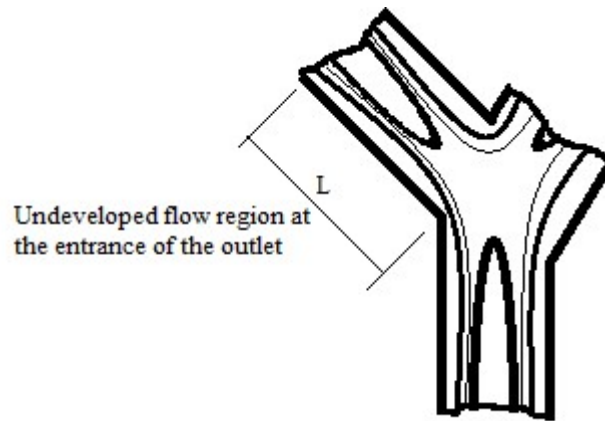


Figure 1. Sketch showing the region of turbulence occurring due to the existence of a bifurcation in a pipe and the length  $L$  of the flow development region at the entrance of one side of the fork (Amado et al, 2018b).

Eq. (2) was assumed as the ideal shape to predict the length of the developing flow region at the entrance of the outlets of bifurcations.

## 3. RESULTS AND DISCUSSION

Figure 2 and 3 show images obtained through the above-mentioned commercial code and Fig. 4 shows an analogous image obtained by the finite difference method. The condition represented consists of half-angles  $\theta_1$  and  $\theta_2$  as 30° and 45°, flow rate  $Q$  as  $2.78 \times 10^{-9} \text{ m}^3/\text{s}$  and diameter of 0.03 m. Note that the flow shown in Fig. 2 and 3 has a shape similar to that shown in Fig. 1, in the inlet region of the bifurcation, as well as the flow represented in each of the outlets of Fig. 4 has a format similar to that shown in those figures, validating the simulation in finite difference method.

Table 1, 2 e 3 shows, respectively, results of length measurements in images generated in the simulations, for the bifurcations with variation of angles and flow rates  $Q$ , according Amado et al, 2018a and diameters, raised herein.

For results of Tab.3 analyzed in isolation, Eq. (3) is the best approximation for predicting the extension of the region of interest.

$$L=2.25(2R)^{-0.1}Re^{0.59}Dh^{1.1} \quad (3)$$

According to Amado et all, 2018a, for the first two isolated conditions of variation shown in Tab. 1 and 2, the best equations would be Eq (4) for angular variation and Eq (5) for flow variation.

$$L=0.0061(2R)^{-0.1}Re^{-1.4}Dh^{1.1} \quad (4)$$

$$L=0.23(2R)^{-0.1}Re^{-0.2}Dh^{1.1} \quad (5)$$

Figure 5 shows the measured length values listed in Tab. 3 against those calculated through Eq. (3).

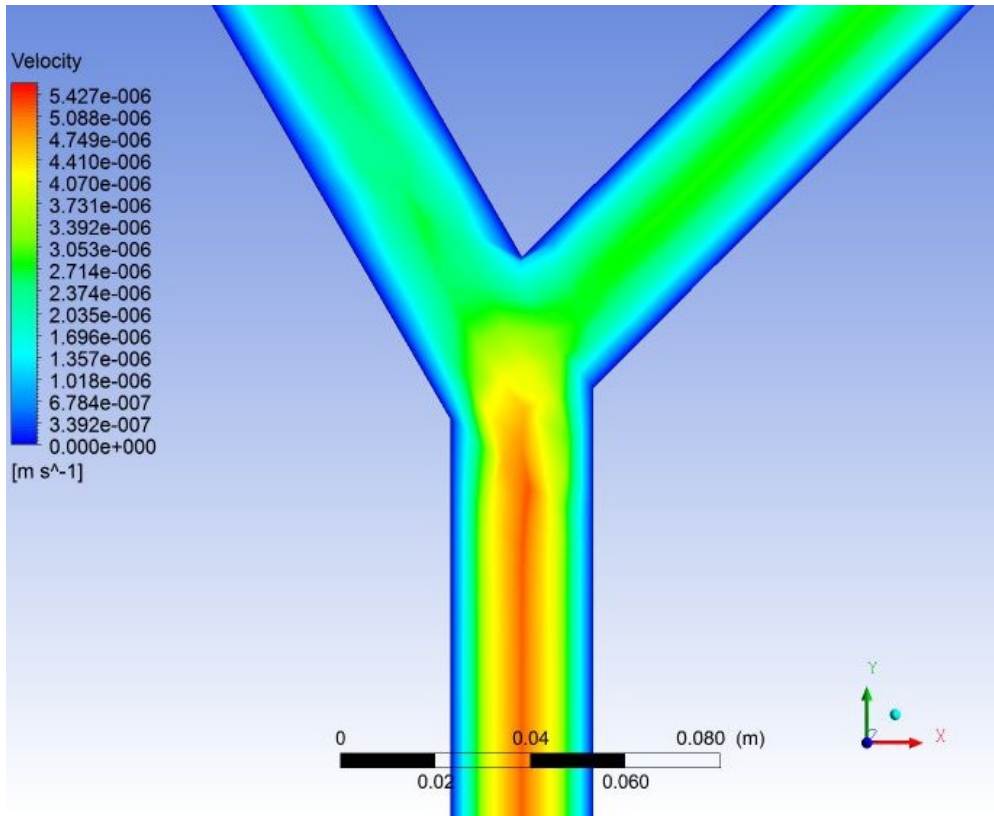


Figure 2. Simulation in commercial code, flow in a bifurcation with half-angles  $\theta_1$  e  $\theta_2$  as 30° and 45°, flow rate  $Q$   $1.39 \times 10^{-9} \text{ m}^3/\text{s}$ , for inlet and outlets with 0.02 m in diameter and 0.9 m of length.

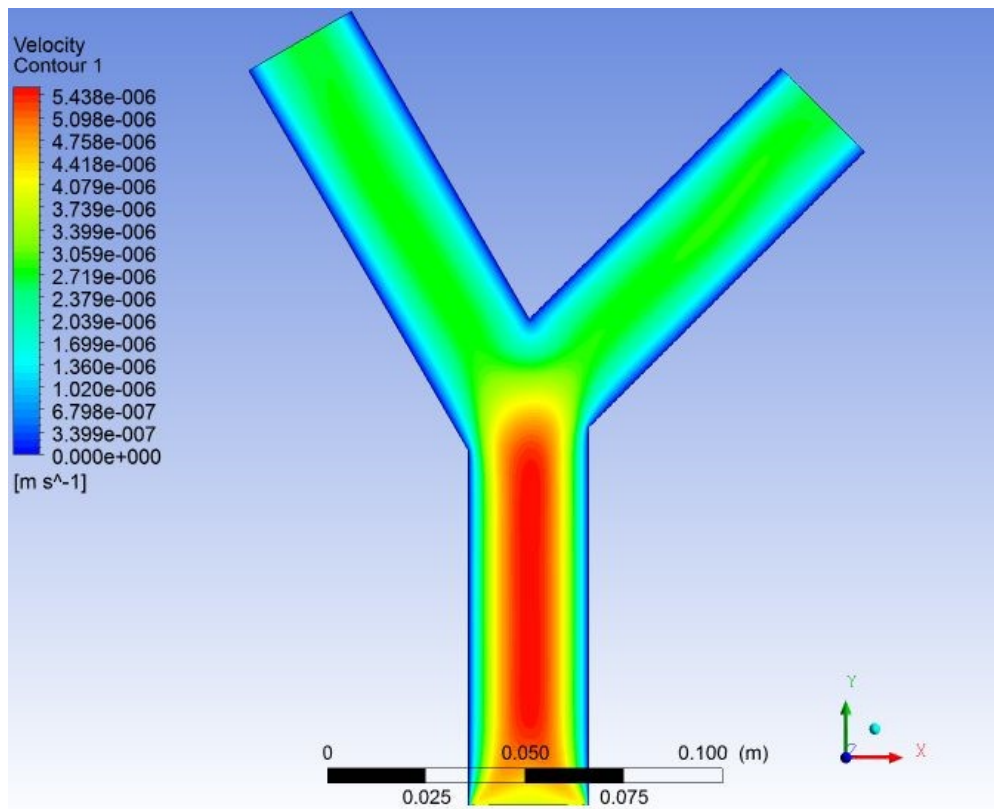


Figure 3. Simulation in commercial code, flow in a bifurcation with half-angles  $\theta_1$  e  $\theta_2$  as 30° and 45°, flow rate  $Q$   $1.39 \times 10^{-9} \text{ m}^3/\text{s}$ , for inlet and outlets with 0.02 m in diameter and 0.09 m of length.

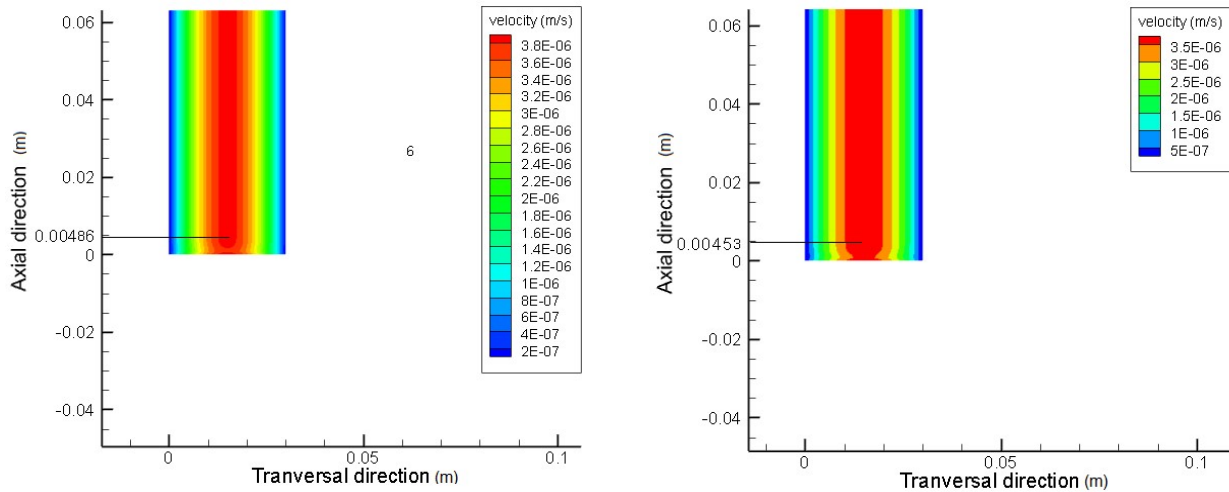


Figure 4. Simulation in finite difference method, flow in a bifurcation with half-angles  $\theta_1$  as  $30^\circ$  at right and  $\theta_2$  as  $45^\circ$  at left, flow rate  $Q$   $2.78 \times 10^{-9} \text{ m}^3/\text{s}$ , for inlet and outlets with 0.03 m in diameter and 0.9 m of length.

Table 1. Values of half-angles and length  $L$  of the not fully developed flow region, measured via CFD, according Amado et al, 2018a.

Bifurcation	Angle (grades)	Diameter and Flow Rates	Length measured (m)
Outlet 1 left	5	0.020 m of diameter and $1.39 \times 10^{-9} \text{ m}^3/\text{s}$ of $Q$ at the feeder channel inlet	0.00303
Outlet 1 right	15		0.00441
Outlet 2 left	15		0.00379
Outlet 2 right	30		0.00455
Outlet 3 left	30		0.00512
Outlet 3 right	45		0.00599
Outlet 4 left	45		0.00558
Outlet 4 right	60		0.00633
Outlet 5 left	60		0.00665
Outlet 5 right	75		0.00735
Outlet 6 left	75		0.00574
Outlet 6 right	90		0.00623

Table 2. Values of flow rate and length  $L$  of the not fully developed flow region, measured via CFD, according Amado et al, 2018a.

Bifurcation	$Q$ ( $\text{m}^3/\text{s}$ )	Angles and Diameters	Length measured (m)
Outlet 1 left	$2.78\text{E}-10$	Half-angles $\theta_1$ e $\theta_2$ as $45^\circ$ and $30^\circ$ and channels with diameters of 0.020 m	0.00453
Outlet 1 right	$2.78\text{E}-10$		0.00433
Outlet 2 left	$3.48\text{E}-10$		0.00552
Outlet 2 right	$3.48\text{E}-10$		0.00477
Outlet 3 left	$5.56\text{E}-10$		0.00519
Outlet 3 right	$5.56\text{E}-10$		0.00446
Outlet 4 left	$6.95\text{E}-10$		0.00559
Outlet 4 right	$6.95\text{E}-10$		0.00375
Outlet 5 left	$9.04\text{E}-10$		0.00512
Outlet 5 right	$9.04\text{E}-10$		0.00362
Outlet 6 left	$1.39\text{E}-09$		0.00453
Outlet 6 right	$1.39\text{E}-09$		0.00387

Table 3. Values of diameter and length of the not fully developed flow region, measured via CFD.

Bifurcation	Diameter (m)	Angles and Flow Rates	Length measured (m)
in	Same as the respective out	Half-angles $\theta_1$ e $\theta_2$ as $45^\circ$ and $30^\circ$ and $2.78 \times 10^{-9}$ $m^3/s$ of $Q$ at the feeder channel inlet	Not measured
Outlet 1 left	0.01		0.00476
Outlet 1 right	0.01		0.00562
Outlet 2 left	0.015		0.00440
Outlet 2 right	0.015		0.00595
Outlet 3 left	0.02		0.00453
Outlet 3 right	0.02		0.00387
Outlet 4 left	0.025		0.00516
Outlet 4 right	0.025		0.00460
Outlet 5 left	0.03		0.00486
Outlet 5 right	0.03		0.00453
Outlet 6 left	0.035		0.00608
Outlet 6 right	0.035		0.00598

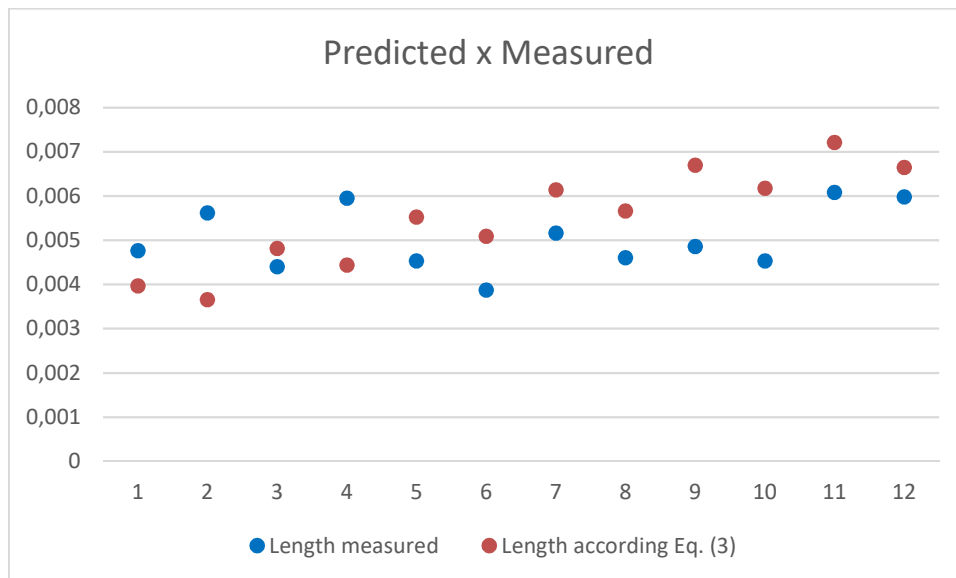


Figure 5. Graphical comparison between values measured by CFD and values predicted by Eq. (3).

Equation (6) adapted for bifurcations of microchannels by Amado et al., 2018b, from the work of Springer et al., 2009, for helicoids and toroids, also fits adequately to the results of diameter variation, maintaining constants half-angles  $\theta_1$  and  $\theta_2$  as  $45^\circ$  and  $30^\circ$  and  $Q$  as  $2.78 \times 10^{-9}$   $m^3/s$  at the feeder channel inlet. Fig. 6 shows the comparison. However, this proposition is not homogeneous from the dimensional point of view and, therefore, escapes the purpose of mathematical rectitude of this work.

$$L=0.161(2R)^{0.3.1}Re^{0.59}Dh^{0.76} \quad (6)$$

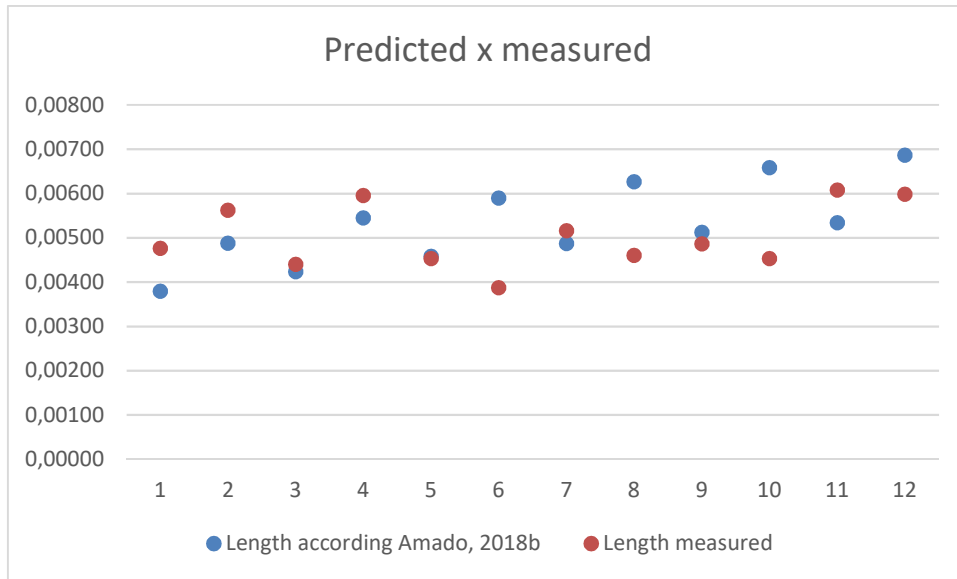


Figure 6. Graphical comparison between values measured by CFD and values predicted by Eq. (6).

The best combination of values of  $k$ ,  $m$ ,  $n$  and  $p$  for an equation covering all values raised in Amado et al, 2018a, and in the present work, would be Eq. (7) below. Figures 7, 8 and 9 show the values of tables 1, 2 and 3 against values calculated by this equation.

$$L = 2.69(2R)^{-0.1} Re^{0.59} Dh^{1.1} \tag{7}$$

For the condition of variation of  $Q$ , maintaining constant angles and diameters, there was some scattering, but in the conditions of variation only of angles or only of diameters, the coincidence was reasonably good.

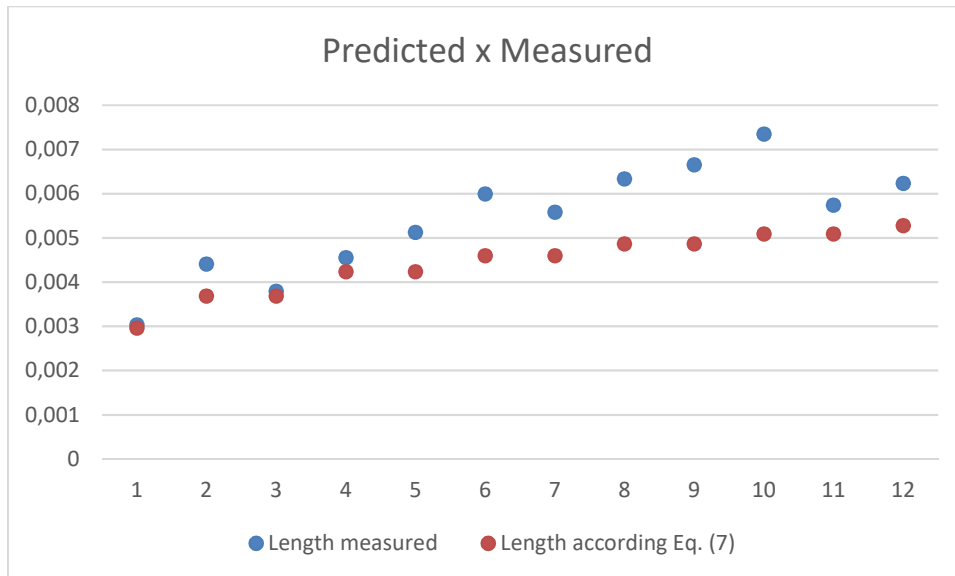


Figure 7. Graphical comparison between values measured by CFD and values predicted by Eq. (7), for angular variation.

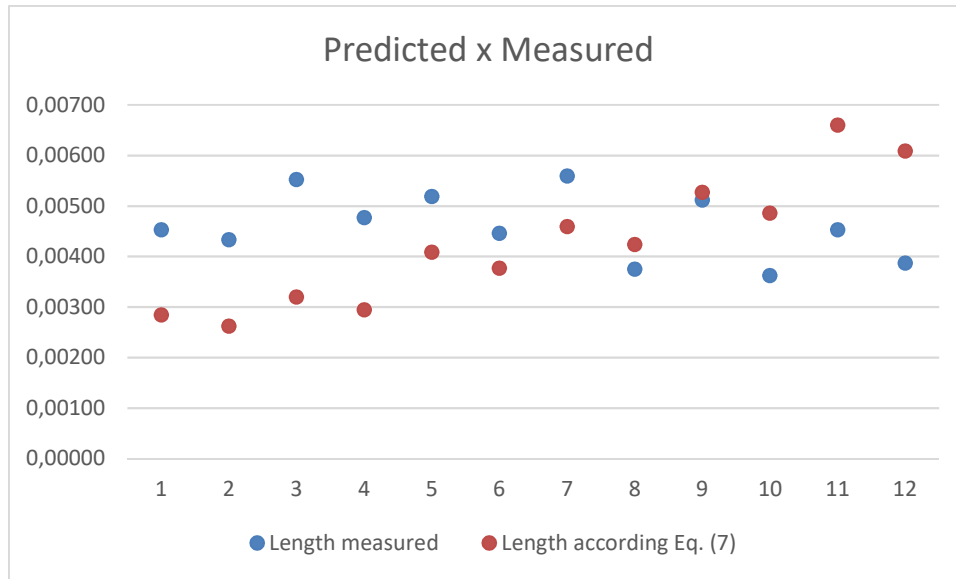


Figure 8. Graphical comparison between values measured by CFD and values predicted by Eq. (7), for flow rate variation.

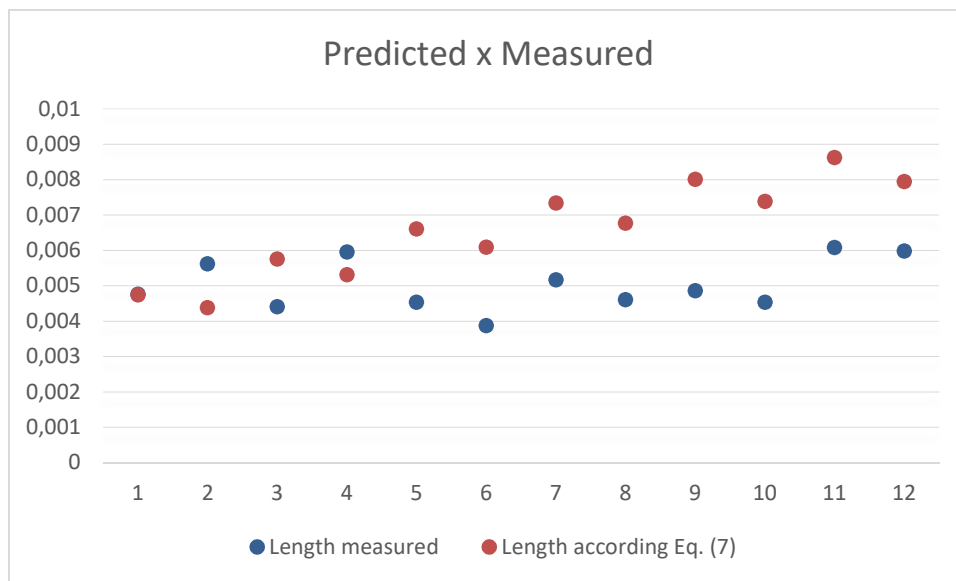


Figure 9. Graphical comparison between values measured by CFD and values predicted by Eq. (7), for variation of diameter.

Equation (7) is dimensionally and physically honest. Dimensionally, because the sum of  $m$  and  $p$  must be equal to 1, which is the exponent of  $L$ , and physically, mainly because it is well known that the larger the diameter of the channel and the radius of curvature of the arc containing the feeder channel and the outlet, the smaller will be  $L$ . Likewise, the larger the Reynolds number, the larger the value of  $L$ , or greater the turbulence at the entrance of the bifurcation.

As a last remark, this work recommends that similar analysis be made to predict the extent of the undeveloped thermal region. Equations found in specialized literature, as presented by Janssen and Hoogendoorn, 1978, or Liu and Masliyah, 1994, can be tested or new models can be postulated. Results of measurement in CFD images can be used for the survey of constants and exponents, as performed in the present work.

#### 4. CONCLUSIONS

Equations of prediction of the flow developing length in asymmetric bifurcations were presented. Expressions shaped as  $L = k (2R)^m Re^n (D)^p$  were employed as the standard format. Values predicted by these equations were compared to values measured in images generated via CFD, performed using the finite difference method.

When varying only diameters  $D$  (from 0.01m to 0.035 m), keeping the flow rate  $Q$  of  $2.78 \times 10^{-9} \text{ m}^3/\text{s}$  and the half-angles of the forks  $\theta_1$  and  $\theta_2$  ( $45^\circ$  and  $30^\circ$ ) as constants,  $L=2.25(2R)^{-0.1}Re^{0.59}Dh^{1.1}$  was the best correlation found. But when all the process variables are taken into account, considering the results presented in Amado et al, 2018a and those presented herein, ( $0.01\text{m} < D < 0.035\text{m}$ ;  $5.56 \times 10^{-10} \text{ m}^3/\text{s} < Q < 2.78 \times 10^{-9} \text{ m}^3/\text{s}$  and  $5^\circ < [\theta_1 \text{ or } \theta_2] < 90^\circ$ ) the best equation was  $L=2.69(2R)^{-0.1}Re^{0.59}Dh^{1.1}$ .

The development of a prediction equation for the thermal entrance length, in a method similar to the present one, is recommended to complete the study of the entrance region in bifurcations.

#### 5. ACKNOWLEDGEMENTS

The authors acknowledge “Programa Pesquisa Produtividade - Universidade Estácio de Sá” for funding the research.

#### 6. REFERENCES

- Agrawal, Y., Talbot, L., and Geong, K., 1978. “Laser Anemometer Study of Flow Development on Curved Circular Pipes”. *Journal of Fluid Mechanics*, vol. 85, no. 3, pp. 497–518.
- Amado, F. P., Avelino, M. R., Colman, J., Lucena, E. S., Mazzarela, N. G. S., 2018. “Developing Flow in the inlet Region of Bifurcations in Microchannels with Symmetric Angulation”. *Proceedings of the CONEM 2018*.
- Amado, F. P., Avelino, M. R., Colman, J., Lucena, E. S., Mazzarela, N. G. S., 2018. “Forecasting the Length of The Undevelopment Flow Region in the Inlet of Asymmetric Bifurcations I”. To be published in the *Proceedings of the ENCIT 2018*.
- Austin, L. R., and Seader, J. D., 1974. “Entry Region for Steady Viscous Flowing Coiled Circular Pipes”. *American Institute of Chemical Engineers*, vol. 20, pp. 820–822.
- Janssen, L. A. M., and Hoogendoorn, C. J., 1978, “Laminar Convection Heat Transfer in Helical Coiled Tubes”. *International Journal of Heat and Mass Transfer*, vol. 21, pp.1197–1206.
- Liu, S., and Masliyah, J. H., 1994. “Developing Convective Heat Transfer in Helical Pipes With Finite Pitch”. *International Journal of Heat and Fluid Flow*, vol. 15, no. 1, pp. 66–75.
- Newson, I. H., and Hodgson, T. D., 1974. “The Development of Enhanced Heat Transfer Condenser Tubing”. *Atomic Energy Research Establishment*, vol. 14, no. 3, pp. 291–323.
- Springer F, Carretier E, Veyret D and Moulin, P., 2009. “Developing Lengths in Woven and Helical Tubes with Dean Vortices Flows”. *Engineering Applications of Computational Fluid Mechanics*, 3:1, 123-134, DOI:10.1080/19942060.2009.11015259.
- Soh, W. Y., and Berger, S. A., 1984. “Laminar Entrance Flow in a Curved Pipe”. *Journal of Fluid Mechanics*, vol. 148, pp. 109–135.
- So, R. M., Zhang, H. S., and Lai, Y. G., 1991. “Secondary Cells and Separation in Developing Laminar Curved-Pipe Flows”. *Theoretical and Computational Fluid Dynamics*, vol. 3, no. 3, pp. 141–162.
- Yao, L. S., and Berger, S.A., 1975. “Entry Flow in a Curved Pipe”. *Journal of Fluid Mechanics*, vol. 67, no. 1, pp. 177–196.

#### 7. RESPONSIBILITY NOTICE

The authors are the only responsible for the printed material included in this paper.